Wrinkling Hierarchy in Constrained Thin Sheets from Suspended Graphene to Curtains

Hugues Vandeparre,[1] Miguel Piñeirua,[2] Fabian Brau,[1] Benoit Roman,[2] José Bico,[2] Cyprien Gay,[3] Wenzhong Bao,[4]
Chun Ning Lau,[4] Pedro M. Reis,[5] and Pascal Damman[1,*]

[1]*Laboratoire Interfaces et Fluides Complexes, CIRMAP, Université de Mons, 20 Place du Parc, B-7000 Mons, Belgium*
[2]*PMMH, CNRS UMR 7636, ESPCI, Paris-Tech, Univ. Paris 6 and Paris 7, 10 Rue Vauquelin, 75231 Paris Cedex 05, France*
[3]*Matière et Systèmes Complexes, Université Paris Diderot—Paris 7, CNRS, UMR 7057, Bâtiment Condorcet,
F-75205 Paris cedex 13, France*
[4]*Department of Physics and Astronomy, University of California, Riverside, California 92521, USA*
[5]*Departments of Mechanical Engineering and Civil and Environmental Engineering, Massachusetts Institute of Technology,
Cambridge, Massachusetts 02139, USA*
(Received 23 February 2011; published 2 June 2011)

We show that thin sheets under boundary confinement spontaneously generate a universal self-similar hierarchy of wrinkles. From simple geometry arguments and energy scalings, we develop a formalism based on *wrinklons*, the localized transition zone in the merging of two wrinkles, as building blocks of the global pattern. Contrary to the case of crumpled paper where elastic energy is focused, this transition is described as smooth in agreement with a recent numerical work [R. D. Schroll, E. Katifori, and B. Davidovitch, Phys. Rev. Lett. **106**, 074301 (2011)]. This formalism is validated from hundreds of nanometers for graphene sheets to meters for ordinary curtains, which shows the universality of our description. We finally describe the effect of an external tension to the distribution of the wrinkles.

The drive towards miniaturization in technology is demanding for increasingly thinner components, raising new mechanical challenges [1]. Thin films are, however, unstable to boundary or substrate-induced compressive loads: moderate compression results in regular wrinkling [2–6] while further confinement can lead to crumpling [7,8]. Regions of stress focusing can be a hindrance, acting as nucleation points for mechanical failure. Conversely, these deformations can be exploited constructively for tunable thin structures. For example, singular points of deformation dramatically affect the electronic properties of graphene [9].

Here, we show that thin sheets under boundary confinement spontaneously generate a universal self-similar hierarchy of wrinkles, from strained suspended graphene to ordinary hanging curtains. We develop a formalism based on *wrinklons*, a localized transition zone in the merging of two wrinkles, as building blocks to describe these wrinkled patterns.

To illustrate this hierarchical pattern, in Fig. 1(a), we show a wrinkled graphene sheet along with an ordinary hanged curtain. These patterns are also similar to the self-similar circular patterns first reported by Argon *et al.* for the blistering of thin films adhering on a thick substrate [10]. The diversity and complexity of those systems, characterized by various chemical and physical conditions, could suggest, *a priori*, that the underlying mechanisms governing the formation of these patterns are unrelated. However, these systems can be depicted, independently from the details of the experiments, as a thin sheet constrained at one edge while the others are free to adapt their morphology. These constraints can take the form of an imposed wavelength at one edge or just the requirement that it should remain flat.

At first sight, as quoted by numerous authors [8,10–16], these patterns consist of a hierarchy of successive generations of folds whose typical size gradually increases along x [Fig. 1(b)]. We propose to rationalize these various hierarchical patterns by considering the evolution of the average wavelength λ with the distance to the constrained edge x. This evolution is adequately described by a simple power law, $\lambda \sim x^m$, see Fig. 1(c), which confirms the self-similarity of these patterns as hypothesized in previous theoretical studies [8,11–13]. Interestingly, curtains made of various materials with contrasted properties exhibit similar exponents. We observe values close to 2/3 for "light" sheets and to 1/2 for "heavy" sheets (both cases defined and discussed in more detail below). Therefore the exponent m is a robust feature of these folding patterns.

In this work, we describe in terms of simple scaling laws the theoretical arguments developed in the mathematical studies of the von Kármán equation [8,12,13,15] and infer the properties of the hierarchical patterns. We also compare these results with extensive experimental data. To the best of our knowledge, the experimental characterization of these patterns had not been carried out to date.

Assuming inextensibility of the sheet along the y direction, the imposed undulation along this direction exactly compensates for an effective lateral compression of the membrane by a factor $(1 - \Delta)$ defined as $(1 - \Delta) \equiv W/W_0 = W/\int_0^W \sqrt{1 + (\partial z/\partial y)^2}\,dy$, where W_0 and W are the curvilinear and projected widths of the curtain, respectively, and $z(x, y)$ is the out-of-plane deformation
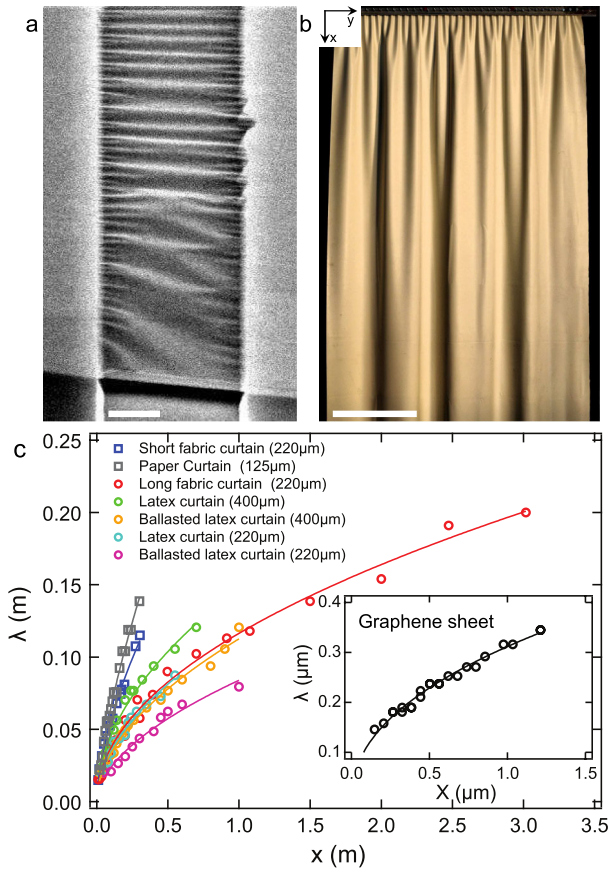
FIG. 1 (color online).　(a) Scanning electron microscopy image of suspended graphene bilayer (scale bar is 1 μm). (b) Pattern of folds obtained for a rubber curtain (scale bar is 25 cm). (c) Evolution of the wavelength λ with the distance from the constrained edge x for various curtains. Power-law fits are added (the power exponents m are close to 2/3 for the short fabric and the paper curtains and 1/2 for the long fabric, the rubber curtains, and the graphene sheet). Inset: Evolution of λ with x for the graphene bilayer. The experimental parameters are detailed in the supplemental information [22].

FIG. 2 (color online).　(a) Schematic representation of the wrinklon experiments. (b) Morphology of the transition λ to 2λ for a constrained plastic sheet for $A = 6$ mm and $\lambda = 8$ mm. (c) Evolution of the normalized length of a wrinklon, L/λ, with the normalized amplitude, A/h (fixed wavelength, $\lambda = 8$ mm), for different thicknesses as indicated.

of the sheet. At any position along the x axis, the function $z(x, y)$ is typically sinusoidal along y, with an amplitude $A(x)$ and a wavelength $\lambda(x)$. The inextensibility hypothesis along the y axis imposes $\Delta \sim (A/\lambda)^2$ at the lowest order, where the lateral compression is assumed to be constant throughout the length of the curtain. The undulations of the sheet along y are characterized by a curvature $\kappa \simeq \partial^2 z/\partial y^2$ whose typical value, varying along x, is of order $\kappa(x) \sim A/\lambda^2$. The corresponding energy per unit area, u_b, for bending the membrane is thus of order $u_b \sim Eh^3\kappa^2 \sim Eh^3\Delta/\lambda^2$, where E is the Young modulus and h the thickness of the sheet. Since u_b is proportional to $1/\lambda^2$, the membrane adopts the largest possible wavelengths, in order to minimize energy. This tendency to increase the wavelength, combined with the constraint imposed at the boundaries, is the source of the observed hierarchical wrinkling pattern.

Inspired by previous models based on successive period-doubling transitions [8,13,17], we consider that the
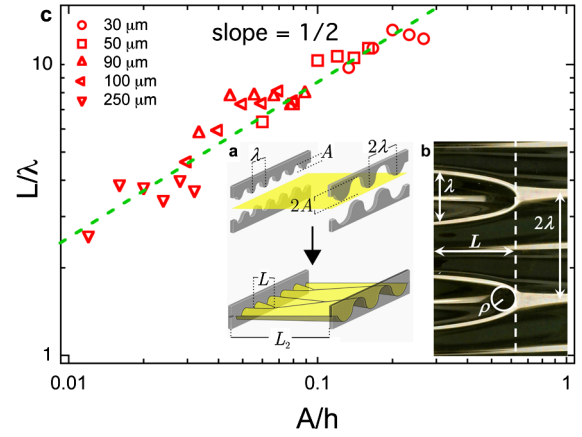
allometric laws mentioned above can be derived by considering that the global pattern results from the self-assembly of building blocks which we denote as wrinklons. A single wrinklon corresponds to the localized transition zone needed for merging two wrinkles of wavelength λ into a larger one of width 2λ. This transition requires a distortion of the membrane which relaxes over a distance L. In other words, each wrinklon is characterized by a size, L, which depends on the material properties and on the wavelength λ. To investigate the properties and behavior of wrinklons, we have performed model experiments using thin plastic sheets. The sheets were constrained with sinusoidal clamps: two opposite edges are constrained by a wavelength λ (amplitude A) and 2λ (amplitude $2A$), respectively; see Figs. 2(a) and 2(b). The normalized size of the wrinklons, L/λ, is plotted in Fig. 2(c) as a function of the normalized amplitude, A/h, the data collapse on a single curve defined by $L/\lambda \sim \sqrt{A/h}$. This relation implies that $L \propto \lambda^{3/2}$ since $A \sim \lambda\sqrt{\Delta}$.

In a further step, the wrinklons can be assembled to mimic the behavior of a complete hierarchy. Indeed, if L is the distance over which the wavelength increases from λ to 2λ, its variation, $d\lambda/dx$, is thus of order λ/L. Hence, the evolution of λ as a function of the distance from the constrained edge x is given by

$$\frac{d\lambda}{dx} \simeq \frac{\lambda}{L}. \tag{1}$$

Considering the scaling $L \propto \lambda^{3/2}$ deduced from the single wrinklon experiments, Eq. (1) indicates that the wavelength along the sheet should evolve like $\lambda \propto x^{2/3}$. The excellent agreement between this power law and the experimental data measured for light sheets [Fig. 1(c)] provides strong support to the concept of wrinklons as building blocks. Equation (1) can now be regarded as a

tool that connects the properties of single wrinklons to the features of the full wrinkling-cascade pattern.

We now focus on the description of an elementary building block. For confined thin sheets, stretching deformations are costly as compared to pure bending. The sheet tends to adopt an isometric (developable) shape [7]. However, the only developable solutions compatible with boundary conditions generally include flat domains surrounded by edge or pointlike singularities. These singularities, which focus the elastic energy into narrow regions, have been classified as developable cones [18,19], ridges [7,20], or curved ridges [21]. In our case, the scenario is, however, significantly different: in contrast to crumpling, stretching is smoothly distributed in the transition zone as pointed out recently in numerical simulations of deformed membranes [17]. The necessary stretching required for connecting the periodic patterns can be illustrated by a simple origami model made with a sheet of paper (see supplemental material [22]). The stretching energy can be estimated through the elongation strain of the sheet along x within a transition domain. The typical value of the strain along x is of order α^2, where $\alpha \sim A/L \sim \lambda\Delta^{1/2}/L$ is the average slope of the membrane. The stretching energy thus reads $U_s \sim Eh(\alpha^2)^2L\lambda \sim Eh\lambda^5\Delta^2L^{-3}$.

As observed in Figs. 1 and 2, wrinklons should also include a tip singularity (a small region where Gaussian curvature is large). This singularity can be described as a semicircular fold of radius ρ [Fig. 2(b)]. The energy of these singularities has been derived by Pogorelov [21] in a study of deformed shells. In our context, the energy of such curved folds reads $U_{cf} \sim Eh^{5/2}\alpha^{5/2}\rho^{1/2} \sim Eh^{5/2}\Delta^{5/4}\lambda^{7/2}L^{-3}$, where the radius at the tip of the wrinklon is taken as $\rho \sim \lambda^2/L$ as suggested by the roughly parabolic shape of the crest of the defect [Fig. 2(b)]. Nevertheless, the ratio of the curved fold energy to the stretching energy of the wrinklon, $U_{cf}/U_s \sim (h/A)^{3/2}$, is very small in our experiments: the effect of this concentrated region can therefore be neglected in the following.

The total energy of a wrinklon, of characteristic area $L\lambda$, is thus given by $U_{tot} = U_s + U_b \simeq Eh\lambda^5\Delta^2L^{-3} + Eh^3\Delta L\lambda^{-1}$. The size of a single wrinklon is finally obtained by minimizing U_{tot} with respect to L, yielding

$$L(\lambda) \sim \Delta^{1/4}\lambda^{3/2}h^{-1/2}. \tag{2}$$

This scaling emerges from a balance between bending and stretching energies and was previously reported for other situations, such as the decay length of an imposed curvature in a sheet [20] or the extension of a pinch in a pipe [23]. The scaling for the wavelength describing the whole hierarchical pattern is obtained by integration of Eq. (1) with $L(\lambda)$ given by Eq. (2) and is found to be

$$\frac{\lambda(x)\Delta^{1/6}}{h} \sim \left(\frac{x}{h}\right)^{2/3}. \tag{3}$$

The scaling law, $\lambda \propto x^{2/3}$, is in very good agreement with the observed power laws for light curtains, e.g., made of fabric or paper sheets [Fig. 1(c)]. In addition to yielding the proper exponent, this relation enables the comparison of the data obtained from seemingly disparate systems, over a wide range of length scales and independently of material properties. Figure 3(a) provides a remarkable collapse of the evolution of the wavelengths measured with light curtains and various thin plastic sheets.

Heavy curtains, made from fabric or rubber, and constrained graphene bilayers do not follow this behavior (instead, they obey $\lambda \propto x^{1/2}$). In these experiments, an additional tensile force is acting on the sheet. This tension T is given by the longitudinal tensile strain induced by thermal manipulation in the case of graphene sheets [5] and by gravity for heavy curtains [$T = \rho_c gh(H - x) \sim \rho_c ghH$, where ρ_c, g, h, and H are the density of the curtain, the gravity constant, the thickness, and the height of the curtain]. These systems can also be compared to the cascade of wrinkles observed for compressed thin polystyrene films on an air-water interface [14] since the surface tension of water at the free edges pulls the thin sheet.

The tension exerted along x per unit width imposes an additional stretching energy given by $U_t \sim T\alpha^2L\lambda \sim T\Delta\lambda^3L^{-1}$, and becomes dominant when $U_t > U_s$, that is when $T > Eh^2\Delta/A$. The total energy of the distorted membrane thus becomes $U_{tot} = U_t + U_b$. The length of a wrinklon found from the minimization of U_{tot} is

$$L(\lambda) \sim \frac{\lambda^2}{h}\sqrt{\frac{T}{Eh}}. \tag{4}$$

Similar relations, reflecting a balance between tension and bending energies, were previously proposed for single wavelength patterns in stretched sheets and heavy curtains [3,16]. As expected, the tensile force increases the length of wrinklons for a given wavelength [15]. By integration of Eq. (1) with $L(\lambda)$ given by Eq. (4), we obtain the corresponding spatial evolution of the wavelength along a heavy sheet:

$$\frac{\lambda(x)}{h} \sim \left(\frac{Eh}{T}\right)^{1/4}\left(\frac{x}{h}\right)^{1/2}. \tag{5}$$

This scaling is in excellent agreement with the power laws observed for heavy curtains and graphene bilayers [Fig. 1(c)]. The data of various macroscopic curtains, graphene bilayers, and nanometric polystyrene indeed collapse onto a single master curve without any fitting parameters [see Fig. 3(b)]. Our formalism is thus validated from hundreds of nanometers for graphene sheets to meters for rubber and fabric curtains, which shows the universality of our description. The transition between the stretching and tension regimes can be obtained by comparing the relations (3) and (5). The critical distance from the edge at which this transition occurs is given by $x^\star/h \sim (Eh/T)^{3/2}\Delta$. In gravity dominated systems, the tension $T \simeq \rho ghH$ gives the typical curtain length $H_c \sim h(E/\rho gh)^{3/5}\Delta^{2/5}$ above which tension dominates. Curtains shorter than H_c (about 1 m for our fabric) were
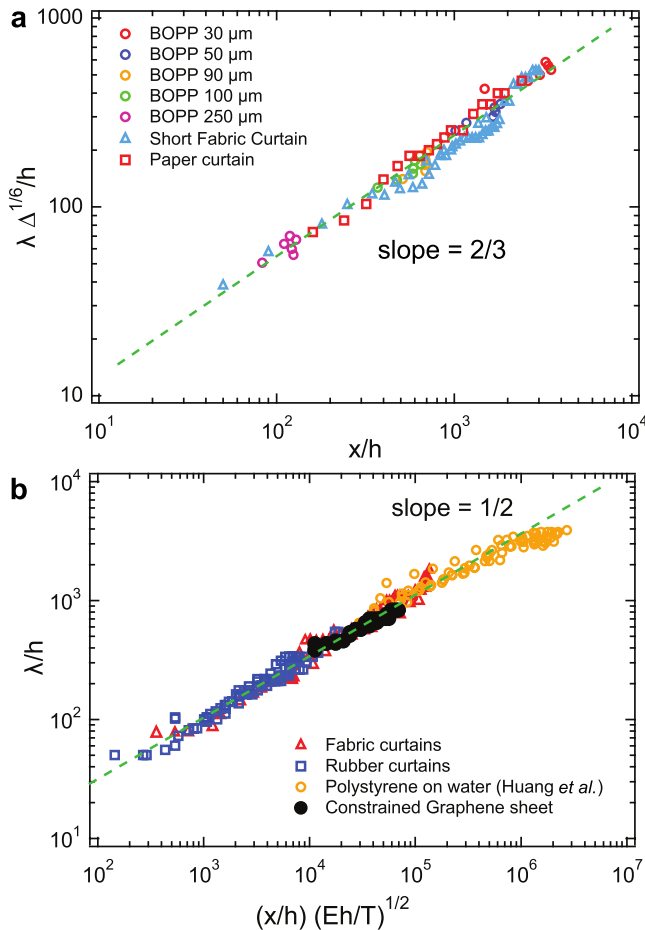
FIG. 3 (color online). Master curves gathering all data. (a) Normalized wavelength, $\tilde{\lambda} = \lambda \Delta^{1/6}/h$, as a function of the normalized distance, $\tilde{x} = x/h$, from the constrained edge for short light sheets (fabric curtain, paper curtain, and constrained plastic sheets). Dashed line: $\tilde{\lambda} = 2.89 \tilde{x}^{0.65}$. (BOPP, biaxially oriented polypropylene). (b) Normalized wavelength $\tilde{\lambda} = \lambda/h$ as a function of the normalized distance from the constrained edge $\tilde{x} = (x/h)(Eh/T)^{1/2}$ for sheets under tension: fabric curtains, rubber curtains, suspended bilayer graphene sheet, and polystyrene thin films deposited on water from Ref. [14]. Dashed line: $\tilde{\lambda} = 2.85 \tilde{x}^{0.52}$.

used to observe the regimes dominated by stretching ("light sheets"), whereas the top part of longer curtains was used for experiments concerning "heavy sheets."

In summary, we showed that the self-similar patterns observed in sheets constrained at one edge cannot be described with d-cone or ridge singularities. In contrast, they can be built by stitching together building blocks, which we call wrinklons, characterized by a diffuse stretching energy. The self-similar structure is then related to the size of these wrinklons that depends on material properties and the local wavelength. Interestingly, we also show that these building blocks can be readily manipulated through the size and energy cost of a single wrinklon by applying a tension. For large values of tension, we even expect a transition towards a purely cylindrical pattern along the sheet with a single wavelength. Finally, we can draw a parallel with the fractal buckling of torn plastic sheets where, in contrast, the different modes are superimposed [24].

*pascal.damman@umons.ac.be

[1] J. A. Rogers and Y. Huang, Proc. Natl. Acad. Sci. U.S.A. **106**, 10 875 (2009).
[2] N. Bowden et al., Nature (London) **393**, 146 (1998).
[3] E. Cerda and L. Mahadevan, Phys. Rev. Lett. **90**, 074302 (2003).
[4] L. Pocivavsek et al., Science **320**, 912 (2008).
[5] W. Bao et al., Nature Nanotech. **4**, 562 (2009).
[6] F. Brau et al., Nature Phys. **7**, 56 (2010).
[7] T. A. Witten, Rev. Mod. Phys. **79**, 643 (2007).
[8] B. Audoly and Y. Pomeau, Elasticity and Geometry: From Hair Curls to the Nonlinear Response of Shells (Oxford University Press, Oxford, 2010).
[9] V. M. Pereira et al., Phys. Rev. Lett. **105**, 156603 (2010).
[10] A. S. Argon et al., J. Mater. Sci. **24**, 1207 (1989).
[11] M. Ortiz and G. Gioia, J. Mech. Phys. Solids **42**, 531 (1994).
[12] S. Conti, A. DeSimone, and S. Müller, Comput. Methods Appl. Mech. Eng. **194**, 2534 (2005).
[13] W. Jin and P. Sternberg, J. Math. Phys. (N.Y.) **42**, 192 (2001).
[14] J. Huang et al., Phys. Rev. Lett. **105**, 038302 (2010).
[15] B. Davidovitch, Phys. Rev. E **80**, 025202(R) (2009).
[16] E. Cerda, L. Mahadevan, and J. M. Pasini, Proc. Natl. Acad. Sci. U.S.A. **101**, 1806 (2004).
[17] R. D. Schroll, E. Katifori, and B. Davidovitch, Phys. Rev. Lett. **106**, 074301 (2011).
[18] M. Ben Amar and Y. Pomeau, Proc. R. Soc. A **453**, 729 (1997).
[19] E. Cerda et al., Nature (London) **401**, 46 (1999).
[20] A. E. Lobkovsky and T. A. Witten, Phys. Rev. E **55**, 1577 (1997).
[21] A. V. Pogorelov, Bendings of Surfaces and Stability of Shells, Translations of Mathematical Monographs Vol. 72 (American Mathematical Society, Providence, 1988).
[22] See supplemental material at http://link.aps.org/supplemental/10.1103/PhysRevLett.106.224301 for experimental section and details about the wrinklon morphology.
[23] L. Mahadevan, A. Vaziri, and M. Das, Europhys. Lett. **77**, 40 003 (2007).
[24] E. Sharon et al., Nature (London) **419**, 579 (2002).